Weak paramagnetism in compounds of the type $Cp'_2Yb(bipy)$†

Marc D. Walter, Madeleine Schultz and Richard A. Andersen*

Received (in Montpellier, France) 12th September 2005, Accepted 13th December 2005
First published as an Advance Article on the web 6th January 2006
DOI: 10.1039/b512865j

Measuring the magnetic moments of solids that are air and moisture sensitive is difficult, particularly when the net magnetic moments are small, as is the case for the organometallic compounds described here. The use of quartz tubes to contain the compounds has been developed and applied to substituted ytterbocene bipyridine complexes, some of which were previously reported as diamagnetic. The SQUID measurements quantify the extent of paramagnetism and they correlate with the qualitative variable temperature ^{1}H NMR spectra.

Introduction

We have previously reported that the tetrasubstituted ytterbocenes $[1,3\text{-}(Me_3C)_2C_5H_3]_2Yb$ and $[1,3\text{-}(Me_3Si)_2C_5H_3]_2Yb$ form diamagnetic 2,2′-bipyridine adducts in the solid state, as determined by SQUID measurements, while other substituted ytterbocenes form weakly paramagnetic complexes in which spin coupling occurs.[1] The SQUID measurements were supported by X-ray crystallography and IR spectroscopy, but the ^{1}H NMR spectrum of $[1,3\text{-}(Me_3C)_2C_5H_3]_2Yb(bipy)$ exhibits broadened and shifted resonances, and its UV spectrum contains the signatures of the bipyridine radical anion, so the characterisation of this "diamagnetic" complex in solution did not agree with what was observed in the solid state.

Our previously reported SQUID measurements were performed in the usual manner using KEL-F buckets to contain the powdered air- and moisture-sensitive sample.[2] Magnetic measurements obtained using such containers are valid when the moments are reasonably high ($\mu_{eff} \approx 1.7\ \mu_B$), but they give rise to uncertainties when the moments are low ($\mu_{eff} \approx 1\ \mu_B$), because the corrections for the container are as large or larger than the measured moments. In addition, in some cases the precise location of the sample is lost with respect to the SQUID pickup coils when the moment is very low. To overcome these problems we have now developed the use of quartz tubes to hold samples within the SQUID magnetometer. As well as minimizing the sample container correction, an additional advantage of the "quartz tube technology" is that it allows the collection of magnetic susceptibility data at temperatures as high as 800 K. The usefulness and accuracy of this method has been confirmed by repeating measurements on known compounds (see later), and by measuring the magnetism of some cerium complexes.[3]

Using the "quartz tube technology", the reported ytterbocene bipyridine complexes have been reinvestigated, along with several new, related compounds, and the results are described in this manuscript. The two tetrasubstituted ytterbocene bipyridine complexes are both found to be weakly paramagnetic, consistent with the solution phase measurements for $[1,3\text{-}(Me_3C)_2C_5H_3]_2Yb(bipy)$. The solid state SQUID and solution ^{1}H NMR and UV-Vis spectroscopic studies provide a unified and consistent picture regarding the extent of paramagnetism in these neutral $Cp'_2Yb(bipy)$ compounds.

Results and discussion

Syntheses and characterisation

The parent compound, $(C_5H_5)_2Yb(bipy)$, is prepared by reaction of KC_5H_5 with YbI_2 in THF followed by addition of the filtrate to a stoichiometric amount of 2,2′-bipyridine, without isolating the initially-formed ytterbocene complex [eqn (1)]. This compound is only sparingly soluble in aliphatic and aromatic solvents, but can be recrystallised from hot THF.

$$KC_5H_5 + YbI_2 \xrightarrow{THF} (C_5H_5)_2Yb \cdot n\mathrm{THF} \xrightarrow{bipy} (C_5H_5)_2Yb(bipy) \qquad (1)$$

Base-free hexasubstituted ytterbocenes bearing bulky trimethylsilyl or *tert*-butyl groups are easily prepared by the reaction of YbI_2 with the sodium salt of the corresponding cyclopentadienyl ligand. Coordinated tetrahydrofuran is lost on exposure to dynamic vacuum, as already reported for $[1,2,4\text{-}(Me_3C)_3C_5H_2]_2Yb$.[4] Both of these base-free molecules sublime in vacuum, and they are readily soluble in aliphatic solvents from which they may be crystallised. They react with 2,2′-bipyridine to yield hexasubstituted ytterbocene 2,2′-bipyridine adducts in good yield [eqn (2)].

$$\begin{aligned} &NaCp' + YbI_2 \\ &\quad \xrightarrow{THF} Cp'_2Yb \cdot THF \\ &\quad \xrightarrow{Vac} Cp'_2Yb \xrightarrow{bipy} Cp'_2Yb(bipy) \\ &Cp' = 1,2,4\text{-}(Me_3Si)_3C_5H_2;\ 1,2,4\text{-}(Me_3C)_3C_5H_2 \end{aligned} \qquad (2)$$

These complexes have been included for the sake of completeness, but they also anchor this study in two directions: the *tert*-butyl substitution provides significant steric bulk around the metal centre, but its electron donating properties should also

---

Chemistry Department and Chemical Sciences Division of Lawrence Berkeley National Laboratory, University of California, Berkeley, California 94720, USA. E-mail: raandersen@lbl.gov; Tel: +1 510 642 4452

† Electronic supplementary information (ESI) available: Magnetic susceptibility *vs.* *T* plots, variable temperature NMR studies and equilibrium thermodynamic data. See DOI: 10.1039/b512865j

stabilise the Yb^{3+} oxidation state, whereas trimethylsilyl substituents, with their electron withdrawing properties, stabilise the Yb^{2+} oxidation state.[5] Although substituent effects on substituted cyclopentadienyl ligands are somewhat controversial, a thorough study of zirconocene derivatives shows that a Me_3C group is a better donor than a Me_3Si group.[6] In addition, the substituent effects deduced for the zirconocenes are in accord with deductions based on the change in the hyperfine coupling constants obtained for the substituted cyclopentadienyl radicals.[7–9]

The bipyridine adduct of the *ansa*-ytterbocene, {*ansa*-[2,4-$(Me_3C)_2C_5H_2]_2SiMe_2$}Yb, was prepared by stirring the diethyl ether adduct[10] with bipyridine. It has similar physical properties to the non-tethered complex $[1,3\text{-}(Me_3C)_2C_5H_3]_2Yb$(bipy).[1]

Some physical characteristics of the new bipyridine complexes are collected in Table 1, along with those of the reported tetrasubstituted compounds that have been reinvestigated. All of the molecules in Table 1, except $[1,2,4\text{-}(Me_3Si)_3C_5H_2]_2Yb$(bipy), are paramagnetic in solution as determined qualitatively by ^1H NMR spectroscopy, since they exhibit broadened and shifted resonances, some of which are temperature dependent; the degree of broadening and shifting varies among the compounds as described in more detail below. The values in Table 1 for μ_{eff} were determined by SQUID magnetometry collected in quartz tubes, as described in the experimental section.

None of the complexes in Table 1 has an absorption in its infrared spectrum around 942 cm^{-1} identifying the reduced bipy radical anion; instead, they have an absorption at 1594 cm^{-1}, which has been used to identify the bipyridine ligand as neutral.[11] The infrared criterion is necessarily qualitative since the interpretation is based on the presence of features rather than their intensity, which can be misleading.

Solid state studies: magnetic susceptibility (SQUID)

An experimental proof of our contention that the magnetic susceptibility data obtained on compounds with relatively high magnetic moments contained in KEL-F buckets or quartz tubes is not significantly different is illustrated in Fig. 1 and 2. Fig. 1 shows the μ_{eff} *vs.* T and Fig. 2 shows χ^{-1} *vs.* T plots for $(C_5Me_5)_2Yb$(bipy) when the container is a KEL-F bucket[1] and when the container is a quartz tube (this work). Inspection shows that the curves track each other throughout the temperature regime studied, supporting our contention that the container correction is insignificant when the net moments are high.

On the other hand, Fig. 3 and 4 show similar plots using KEL-F and quartz containers for {*ansa*-[2,4-$(Me_3C)_2C_5H_2]_2SiMe_2$}Yb(bipy). As can be seen, the μ_{eff} *vs.* T plots are parallel, but not superimposable, which implies that the μ_{eff} curves differ by a scaling factor that is presumably due to the size of the container correction. The deviation is more dramatic when the data is presented as a χ^{-1} *vs.* T plot as illustrated in Fig. 4. Fig. 5 shows χ *vs.* T plots for the diamagnetic compound $(MeC_5H_4)_2Fe$ measured in a quartz tube, showing that when Pascal's constants are used to correct the data for the bulk diamagnetism the value of χ is small and negative.[12]

The solid state magnetism of all of the compounds in Table 1 was investigated using the quartz tube technology at 5 and 40 kG. The magnetic moments obtained for these bipyridine adducts are low, ranging from 0.7 to 1.2 μ_B at 300 K.[13] The magnetic data are presented in two different formats in Fig. 6 and 7. The χ^{-1} *vs.* T plots are significantly curved (Fig. 7), but do not exhibit the unusual behaviour shown by $(Me_5C_5)_2Yb$(bipy) and $(Me_4C_5H)_2Yb$(bipy).[1,3] Due to the air sensitivity of these molecules, it could be argued that the low observed moments are due to paramagnetic impurities, and that the complexes are actually diamagnetic (our previous hypothesis). In order to address this point, the effect of a small amount of a Yb(III) ($J = 7/2$) impurity in the calculation was tested. In order to calibrate our own method the behaviour of the diamagnetic $(Me_5C_5)_2Yb(py)_2$, in which Yb has a $4f^{14}$ electron configuration, was investigated by SQUID magnetometry. A mathematical analysis of the χ^{-1} *vs.* T data led to the small moment ($\mu_{eff} \sim 0.3\ \mu_B$ at 300 K) being attributable to an Yb(III) impurity of roughly 0.5% (Fig. 8) (see ESI for the mathematical analysis†). The data in Fig. 6 and 7 are not corrected for such an impurity.

The complex $[1,2,4\text{-}(Me_3Si)_3C_5H_2]_2Yb$(bipy) is the only substituted ytterbocene bipyridine adduct in Table 1 whose SQUID data exhibits features expected for a diamagnetic Yb(II) compound and a small amount of an Yb(III) impurity; that is, the data are essentially superimposable on Fig. 8 and the compound is therefore categorised as diamagnetic. The proportion of paramagnetic impurity calculated is ∼3%, which seems large, but the compound is very soluble and purification is difficult. The value does not become smaller on repeated recrystallisation, which reflects another difficulty in measuring molecules with very small values of μ_{eff}, *viz.* sample purity. The magnetic behaviour of the other complexes, however, cannot be explained by the presence of some oxidised Yb(III) impurity, and the low magnetic moments are attributed to electron exchange coupling.

Solution studies: UV-Vis spectroscopy

The complexes are strongly coloured, and their optical spectra have been investigated to determine whether the signatures due

Table 1 Solid state characteristics of substituted ytterbocene 2,2′-bipyridine complexes

Compound	Colour	Mp (°C)	IR (cm^{-1})	μ_{eff}(300 K) (μ_B)
$(C_5H_5)_2Yb$(bipy)	Dark blue	218–220	1587	1.2
$[1,3\text{-}(Me_3Si)_2C_5H_3]_2Yb$(bipy)[a]	Dark green	208–212	1594	1.1
$[1,2,4\text{-}(Me_3Si)_3C_5H_2]_2Yb$(bipy)	Blue-black	233–238	1595	0.0
$[1,3\text{-}(Me_3C)_2C_5H_3]_2Yb$(bipy)[a]	Blue-green	278–280	1593	0.9
$[1,2,4\text{-}(Me_3C)_3C_5H_2]_2Yb$(bipy)	Dark red	172–178	1598	0.7
{*ansa*-[2,4-$(Me_3C)_2C_5H_2]_2SiMe_2$}Yb(bipy)}	Dark blue	337–338	1594	1.1

[a] From ref. 1.

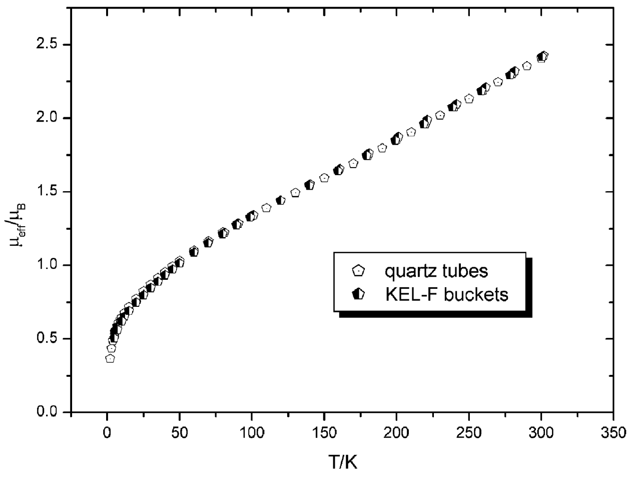

Fig. 1 Solid state magnetic susceptibility, μ_{eff} *vs.* *T* plot of $(Me_5C_5)_2Yb(bipy)$ acquired in quartz tubes and KEL-F buckets.

to reduced or neutral bipyridyl are observed. It has been demonstrated that the bipyridine radical anion has a diagnostic optical spectrum, which is different from that of the colourless, neutral bipyridine, as expected for a species in which the odd electron is located in a π* molecular orbital.[14] These characteristic, strong absorbances, exemplified by Na(bipy), can be compared with the absorbances of the molecules described here. The most notable features for the bipyridine radical anion are transitions between 800–900 nm. The UV-Vis data for the bipyridine complexes are provided in Table 2, along with the data for Na(bipy) and $[1,3\text{-}(Me_3Si)_2C_5H_3]_2Yb(py)_2$.

Fig. 9 shows the optical spectra of the ytterbocene complexes in toluene or methylcyclohexane (mch). The transitions of $(Me_5C_5)_2Yb(bipy)$ have been assigned.[15] It can be seen from Table 2 and Fig. 9 that the spectra of $(C_5H_5)_2Yb(bipy)$, $[1,3\text{-}(Me_3C)_2C_5H_3]_2Yb(bipy)$, $[1,2,4\text{-}(Me_3C)_3C_5H_2]_2Yb(bipy)$ and $\{ansa\text{-}[2,4\text{-}(Me_3C)_2C_5H_2]_2SiMe_2\}Yb(bipy)$ contain the characteristic absorbances due to the bipyridine radical anion, while those of $[1,3\text{-}(Me_3Si)_2C_5H_3]_2Yb(bipy)$, $[1,2,4\text{-}(Me_3Si)_3C_5H_2]_2Yb(bipy)$ and $[1,3\text{-}(Me_3Si)_2C_5H_3]_2Yb(py)_2$ do not.

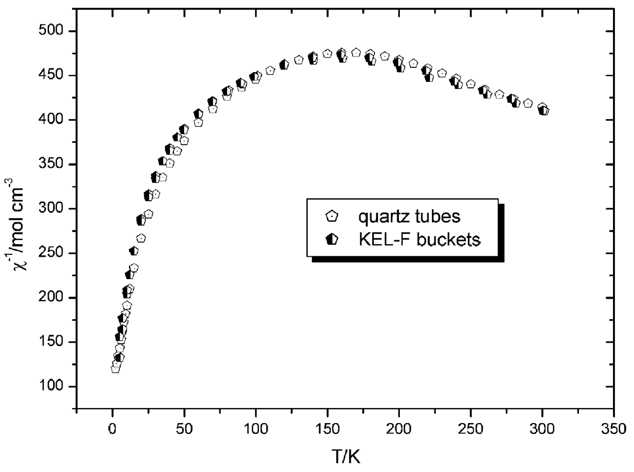

Fig. 2 Solid state magnetic susceptibility, χ^{-1} *vs.* *T* plot of $(Me_5C_5)_2Yb(bipy)$ acquired in quartz tubes and KEL-F buckets.

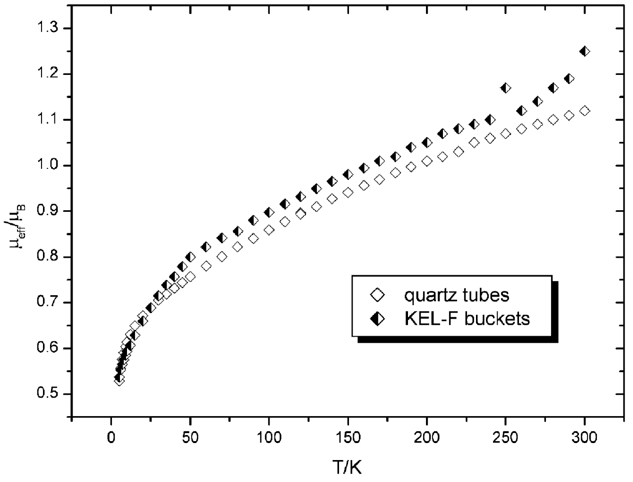

Fig. 3 Solid state magnetic susceptibility, μ_{eff} *vs.* *T* plot of $\{ansa\text{-}[2,4\text{-}(Me_3C)_2C_5H_2]_2SiMe_2\}Yb(bipy)$ acquired in quartz tubes and KEL-F buckets.

The presence of the absorbances characteristic of bipyridine radical anion in the UV spectra of the compounds described here is not consistent with the oxidation state of the bipyridine ligand as deduced from infrared spectroscopy (Table 1), but agrees with the SQUID determinations using the quartz tube method for all compounds other than $[1,3\text{-}(Me_3Si)_2C_5H_3]_2Yb(bipy)$.

Solution studies: ^1H NMR spectroscopy

The ^1H NMR spectrum of any compound, and in particular a lanthanide complex, qualitatively indicates whether the complex is dia- or paramagnetic in solution. This method is extremely sensitive to compounds that are weakly paramagnetic, when the isotropic shifts are large and temperature dependent.[16,17] Unfortunately, the low solubility and the high air sensitivity of the compounds described here did not allow the use of the Evans' method to determine solution moments, and only qualitative inferences are possible.

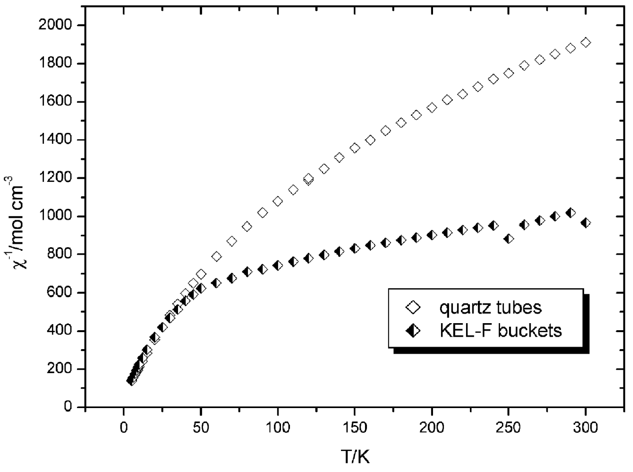

Fig. 4 Solid state magnetic susceptibility, χ^{-1} *vs.* *T* plot of $ansa\text{-}[2,4\text{-}(Me_3C)_2C_5H_2]_2SiMe_2Yb(bipy)$ acquired in quartz tubes and KEL-F buckets.

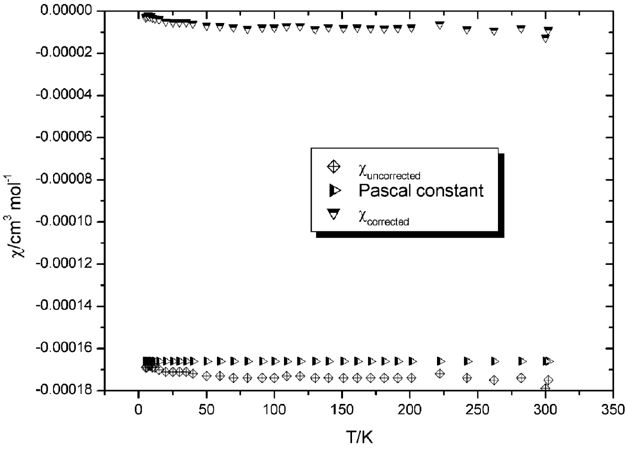

Fig. 5 Solid state magnetic susceptibility, χ *vs.* T plot of $(MeC_5H_4)_2Fe$ acquired in quartz tubes before and after subtracting Pascal constants.

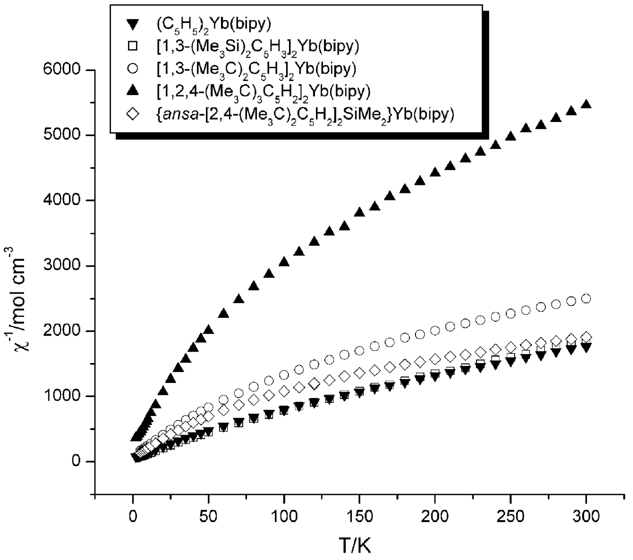

Fig. 7 Solid state magnetic susceptibility, χ^{-1} *vs.* T plot of $Cp'_2Yb(bipy)$ acquired in quartz tubes.

The chemical shifts of the ytterbocene bipyridine compounds are temperature dependent, and ^1H NMR spectra were collected for each bipyridine complex over a range of temperatures, with the exception of $(C_5H_5)_2Yb(bipy)$, due to its low solubility in aromatic hydrocarbon solvents. Other than $[1,2,4-(Me_3Si)_3C_5H_2]_2Yb(bipy)$ (Fig. 10) and $[1,2,4-(Me_3C)_3C_5H_2]_2Yb(bipy)$ (described in more detail below) all ytterbocene bipyridine complexes including those described previously[1] exhibit a temperature dependence of their chemical shifts, but the chemical shifts do not follow Curie–Weiss behaviour; that is, they are non-linear in T^{-1}.

Although the chemical shifts of $[1,3-(Me_3Si)_2C_5H_3]_2Yb(bipy)$ exhibit only small paramagnetic contributions, the bipyridine resonances show temperature dependent non-Curie–Weiss behaviour (Fig. 11). Thus the chemical shift of the most shifted bipyridine proton resonance (δ 13.2 in C_6D_6; δ 13.93 in toluene at 20 °C) moves downfield as the temperature is decreased. This behaviour implies that this molecule is feebly paramagnetic in solution, consistent with the new SQUID measurements, even though signatures due to the bipyridine radical anion are not detected in its UV-Vis spectrum.

The chemical shifts of the chemically inequivalent resonances in $[1,3-(Me_3C)_2C_5H_3]_2Yb(bipy)$ in toluene-d_8 at temperatures from +20 to +90 °C also vary; the plot is provided in the ESI.† The low solubility of this compound in benzene or toluene precludes low temperature measurements, and due to the limited temperature regime no significant deviation from Curie–Weiss behaviour is observed. However, the paramagnetic contribution to the chemical shift is obvious by the range of observed chemical shifts and their temperature dependence. Thus, the chemical shift of the most shifted proton changes from δ 43.9 (C_6D_6) or 49.5 (C_7D_8) at 23 °C to δ 48.4 at 80 °C.

The room temperature ^1H NMR spectrum of $\{ansa\text{-}[2,4-(Me_3C)_2C_5H_2]_2SiMe_2\}Yb(bipy)$ contains nine resonances, consistent with C_2 symmetry. The Me_3C and $SiMe_2$ resonances are readily identified at δ 5.08, 0.69 and −0.05, respectively, on the basis of their relative integrated area

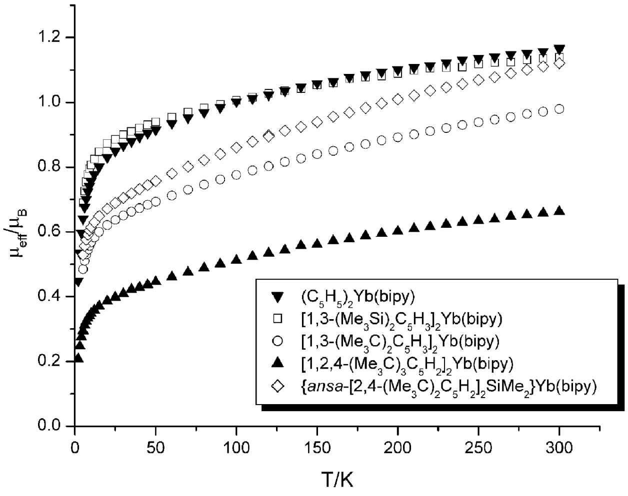

Fig. 6 Solid state magnetic susceptibility, μ_{eff} *vs.* T plot of $Cp'_2Yb(bipy)$ acquired in quartz tubes.

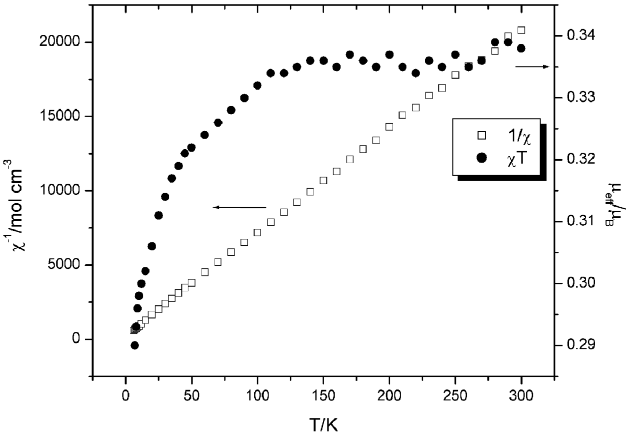

Fig. 8 χ^{-1} *vs.* T and μ_{eff} *vs.* T plots of $(Me_5C_5)_2Yb(py)_2$ acquired in quartz tubes.

Table 2 Optical spectra of 2,2′-bipyridine ytterbocene complexes

Compound	λ_{max} (nm) [$\varepsilon \times 10^{-3}$ (L mol^{-1} cm^{-1})]
$(C_5H_5)_2$Yb(bipy) in toluene	881 [0.42], 850 [0.44], 778 [0.39], 697 [0.30], 493 [0.55], 467 [0.49], 379 [1.57]
$[1,3\text{-}(Me_3Si)_2C_5H_3]_2$Yb(bipy) in toluene[a]	668 [0.41], 392 [1.29]
$[1,2,4\text{-}(Me_3Si)_3C_5H_2]_2$Yb(bipy) in mch	633 [0.27], 392 [0.95]
$[1,3\text{-}(Me_3C)_2C_5H_3]_2$Yb(bipy) in toluene[a]	880 [1.00], 845 [1.06], 767 [1.01], 678 [0.76], 488 [1.91], 465 [1.77], 390 [4.19]
$[1,2,4\text{-}(Me_3C)_3C_5H_2]_2$Yb(bipy) in mch	904 [1.23], 879 [1.29], 854 [1.23], 793 [1.26], 497 [2.29], 477 [2.11], 444 [1.80], 385 [7.69]
{*ansa*-$[2,4\text{-}(Me_3C)_2C_5H_2]_2SiMe_2$}Yb(bipy) in toluene	890 [0.70], 835 [0.73], 779 [0.73], 697 [0.66], 485 [1.10], 461 [1.01], 382 [2.42]
Na(bipy) in THF[b]	952 [1.3], 833 [1.5], 752 [1.1], 562 [6.5], 532 [6.2], 368
$[1,3\text{-}(Me_3Si)_2C_5H_3]_2$Yb(py)$_2$ in toluene[a]	670 [0.17], 401 [0.24]

[a] From ref. 1. [b] From ref. 14.

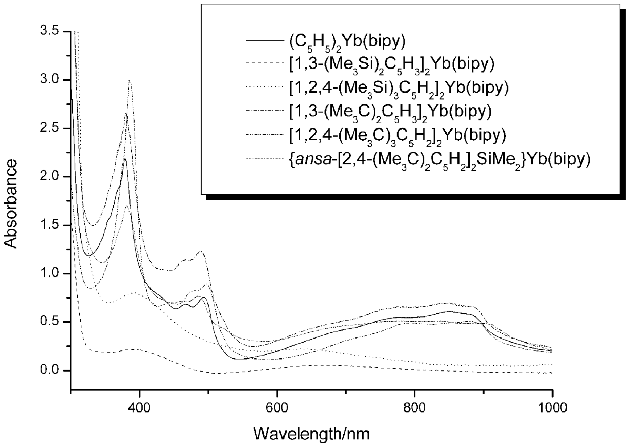

Fig. 9 Optical spectra of Cp'_2Yb(bipy) compounds.

ratios. The other six, equal area resonances are due to the ring and bipyridine protons. Two of the six resonances [δ 14.4 (B) and 3.72 (E)] exhibit resolved coupling, identifying these shifts as bipyridine protons, but a complete assignment of the remaining resonances is not possible because exchange with free bipyridine is slow on the NMR time-scale, since no change in chemical shift is observed upon addition of free bipyridine, which would identify the bipyridine resonances. ^{1}H NMR spectra of the *ansa* compound were collected at temperatures from −70 to +90 °C. A plot of δ *vs.* T^{-1} for the ring methine and bipyridine resonances is shown in Fig. 12, while a stacked plot of the ^{1}H NMR spectra is shown in Fig. 13. The resonances due to the Me_3C and $SiMe_2$ groups are essentially temperature independent, and have not been included in the δ *vs.* T^{-1} plot. Two other resonances at δ 10.1 (C) and 3.72 (E) (20 °C) are only weakly temperature dependent, as can be seen in Fig. 13 and 14. The other four resonances have non-linear temperature dependences; two shift towards the diamagnetic region (δ 28.9 (A), −2.15 (F) at 20 °C) in a monotonic but non-linear manner, while the other two (δ 14.4 (B), 10.1 (D) at 20 °C) shift in a decidedly non-monotonic manner. Clearly these four resonances do not show Curie–Weiss behaviour. The curved lines in the δ *vs.* T^{-1} plots are presumably the superposition of curves due to the two or more species whose relative populations change with temperature. Since free bipyridine does not exchange rapidly with this complex in the temperature range studied (see below), the non-linear temperature dependence must be due to an intramolecular process.

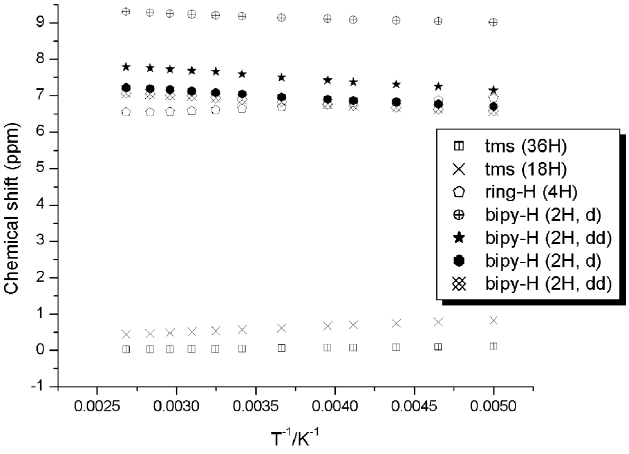

Fig. 10 Chemical shift (δ) *vs.* T^{-1} plot of ^{1}H NMR resonances of $[1,2,4\text{-}(Me_3Si)_3C_5H_2]_2$Yb(bipy) in toluene-$d_8$ at temperatures from 203 K to 373 K.

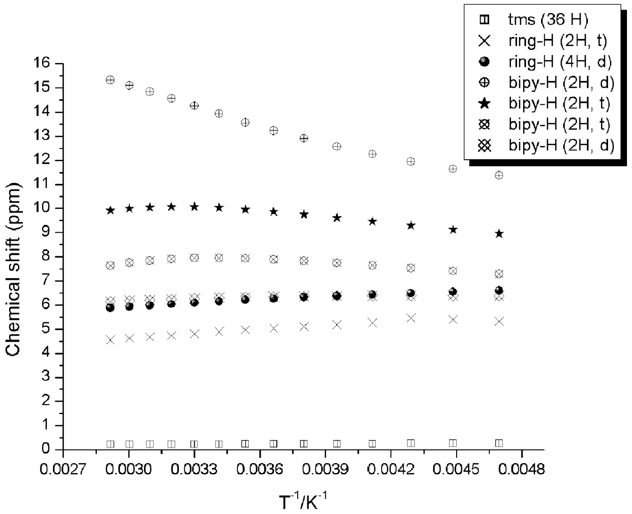

Fig. 11 Chemical shift (δ) *vs.* T^{-1} plot of ^{1}H NMR resonances of $[1,3\text{-}(Me_3Si)_2C_5H_3]_2$Yb(bipy) in toluene-$d_8$ at temperatures from 203 K to 363 K.

The variable temperature ^{1}H NMR spectrum of $[1,2,4\text{-}(Me_3C)_3C_5H_2]_2$Yb(bipy) (Fig. 14) is rather complex but the pattern of the resonances may be understood in the following way. At room temperature (293 K; T^{-1} = 0.0034 K^{-1}) the equilibrium shown in eqn (3) is fast on the NMR timescale.

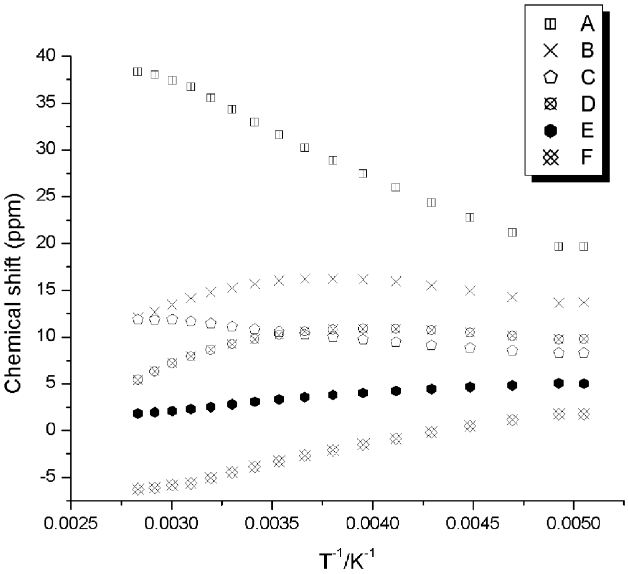

Fig. 12 Chemical shift (δ) *vs.* T^{-1} plot of the bipyridine and methine ^{1}H NMR resonances of {*ansa*-[2,4-$(Me_3C)_2C_5H_2]_2SiMe_2$}Yb(bipy) in toluene-d_8 at temperatures from 203 K to 363 K. The Me_3C and Me_2Si resonances have been omitted for clarity.

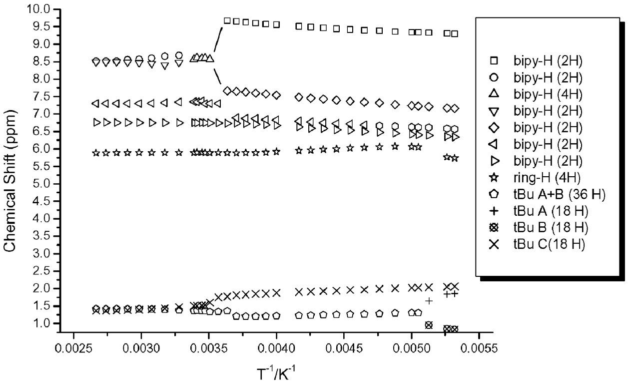

Fig. 14 Chemical shift (δ) *vs.* T^{-1} plot of ^{1}H NMR resonances of $[1,2,4\text{-}(Me_3C)_3C_5H_2]_2Yb(bipy)$ in toluene-d_8 at temperatures from 375 K to 188 K. The resonances corresponding to free bipy and $[1,2,4\text{-}(Me_3C)_3C_5H_2]_2Yb$ have been omitted for clarity.

Thus, the chemical shifts are the averaged values of the individual species in solution. When free bipyridine is added to the solution at 20 °C, all of the resonances shift towards the chemical shifts of the free molecules, as expected when intermolecular exchange is rapid. As the temperature is lowered, the equilibrium moves to the left. The ^{1}H NMR spectra from 290 K (T^{-1} = 0.0034 K^{-1}) to 197 K (T^{-1} = 0.0051 K^{-1}) exhibit resonances for the four bipyridine protons, the Cp ring protons and the Me_3C protons. The Me_3C resonances are in a 2 : 1 area ratio, consistent with rotation about the pseudo C_5 axes of the Cp rings so that the complex has C_{2v} symmetry. Below 197 K, the Me_3C group resonance of area 2 decoalesces, consistent with slowing the rotation or oscillations of the cyclopentadienyl rings and generating a molecule with C_2 (eclipsed) or C_s (staggered) cyclopentadienyl rings. Based on the coalescence temperature of 197 K, $\Delta G^{\ddagger}$ for this equal population two site exchange process is 9 kcal mol^{-1}. This type of fluxional behaviour has been observed in cerium and uranium metallocene complexes with the same substituted cyclopentadienyl ligand.[18,19]

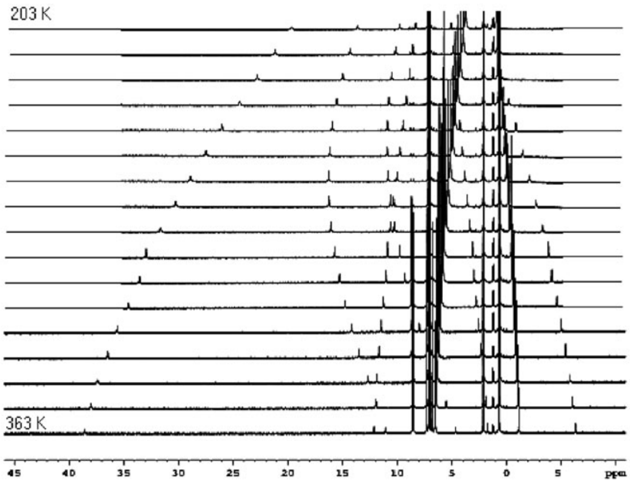

Fig. 13 Stacked plot of ^{1}H NMR spectra of {*ansa*-[2,4-$(Me_3C)_2C_5H_2]_2SiMe_2]_2$}Yb(bipy) in toluene-$d_8$ at temperatures from 203 K to 363 K. Spectra were collected every 10 K, and the plot is from low temperature (top) to high temperature (bottom).

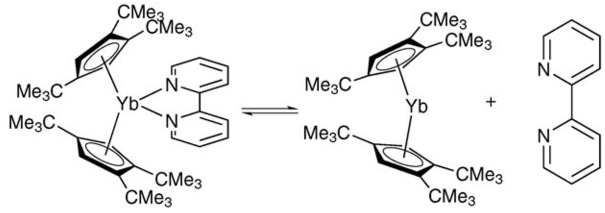

(3)

The thermodynamic parameters for the equilibrium in eqn (3) were obtained over the temperature range 273 K (T^{-1} = 0.0037 K^{-1}) to 218 K (T^{-1} = 0.0046 K^{-1}). At a given temperature, the ratio of the three species (deduced from the integration of the ^{1}H NMR spectrum) is used to calculate K. A plot of ln K *vs.* T^{-1} is linear (see ESI†) and yields ΔH = 10.4 kcal mol^{-1}; ΔS = 36 cal mol^{-1} K^{-1}; $\Delta G_{300\ K}$ = −0.22 kcal mol^{-1}. These quantitative thermodynamic data mean that at 290 K, ΔG is approximately zero and the populations of the free and bound species are approximately equal. As the temperature increases, the free to bound ratio increases; at 300 K (T^{-1} = 0.0033 K^{-1}) the ratio of free to bound is about 3 : 1 and the observed chemical shifts approach their uncomplexed values.

The solution behaviour of $[1,2,4\text{-}(Me_3C)_3C_5H_2]_2Yb(bipy)$ is unique, because it is the only substituted ytterbocene bipyridine adduct exchanging (rapidly) on the NMR time scale (10^{-1}–10^{-9} s) on addition of free 2,2′-bipyridine.[20] The rapid exchange is consistent with our previous report that the $[1,2,4\text{-}(Me_3C)_3C_5H_2]_2Yb$ fragment is sterically crowded so that only one isocyanide ligand binds, in contrast to other ytterbocenes that always bind two isocyanide ligands.[5] Addition of free bipyridine to solutions of all other substituted ytterbocene bipyridine complexes does not affect the positions or line width of the resonances in the ^{1}H NMR spectra, even during variable temperature experiments. This is consistent with the notion that the curvature observed in the δ *vs.* T^{-1} plots is not due to an intermolecular exchange process, but it is related to intramolecular processes, two of which are (a) fluxional motion of the planar bipyridine ligand relative to the molecular z-axis and (b) change in spin coupling that changes the relative population of spin isomers.[3]

Conclusions

The important point that emerges from this study is that measuring the solid state magnetic susceptibility of compounds with low but non-zero values of μ requires extraordinary care. This is particularly true for the compounds described here, since they are air and moisture sensitive and the oxidised form is paramagnetic. The method described and advocated here requires the use of sealed quartz tubes for all magnetic measurements, measurement at two different applied magnetic fields, and where possible comparison with other solution spectroscopic data, particularly the variable temperature NMR spectra. The magnetic susceptibility data as a function of temperature are quantitative and give a measure of the extent of paramagnetism, but the interpretation of its origin is much less clear and is under investigation.[3]

Experimental

Magnetic measurements "quartz tube technology"

Data were collected from 5–300 K at two different field strengths (typically 5 and 40 kG), unless stated otherwise, on a Quantum Design MPMS XL7 SQUID magnetometer. High purity glass wool was initially loaded into small pieces of quartz tubing of 2–3 cm length and a diameter of 3 mm using quartz rods (2 mm diameter, 22 cm long) as plungers. Gloves were required to avoid contamination of the quartz wool during this procedure. All of the loading equipment (quartz sample tubes, quartz wool in short tubes, moulder, plungers, Pasteur pipettes) was then stored in an oven at 250 °C for at least 48 h and was transferred into a N_2 filled glove box immediately prior to use. The quartz sample tubes had a diameter of 3 mm and were 25 cm long which allows low (2–400 K) and high temperature (400–800 K) measurements on one sample. A distance of 3 cm from both ends was reserved for safe sealing and to allow attachment of the vacuum adapters. The sample was located 11 cm from one end of the tube and 14 cm from the other. The sample height including quartz wool did not exceed 1.5 cm. For convenience, a plastic stick carrying the necessary distance marks was used to ensure correct sample placement during the loading procedure in the glove box. The mass of the empty quartz tube before and after every loading step was determined on a balance in the glove box. To load the sample, first one plug of quartz wool was transferred to the sample quartz tube in the following manner: the small piece of quartz tubing carrying the dried quartz wool was positioned at one end of the sample tube and the plug was pushed with a plunger through one tube into the other and placed in the correct position. Contact of the quartz wool with the gloves was avoided. The pulverised sample (typically 15–20 mg) was then transferred *via* a Pasteur pipette into the sample tube. To hold the sample in the correct position during the measurement, a second plug of quartz wool was placed on the top of the pulverised sample in the same manner. The total amount of quartz wool used for this procedure ranged from 4–7 mg. To avoid orientation effects, the sample was tightly packed by compressing it simultaneously with two plungers. Two vacuum adapters were then carefully attached to both ends of the sample tube and the assembly was taken outside the glove box, where it was carefully exposed to dynamic vacuum. Both ends of the sample container were flame sealed and quartz loops were attached to both ends, which were connected *via* platinum wire to the transport rod in the magnetometer. The susceptibility data were corrected for diamagnetic contributions of the sample using Pascal constants[12] and for the quartz wool background. For this reason a series of quartz tubes carrying only different amounts of quartz wool were measured and a mathematical fit depending on the quartz wool mass was subsequently applied.

Syntheses

$(C_5H_5)_2$Yb(bipy). The potassium salt K(C_5H_5) (1.40 g, 13.5 mmol) and YbI_2 (3.30 g, 7.7 mmol) were weighed together into a Schlenk flask equipped with a magnetic stirrer under a flow of nitrogen. Tetrahydrofuran (60 mL) was added and the bright purple slurry was stirred overnight at room temperature. 2,2′-Bipyridine (1.20 g, 7.6 mmol) was weighed into a clean Schlenk flask and the purple THF solution of $(C_5H_5)_2$Yb(THF)$_2$ was filtered into that flask. The solution became dark green-blue upon contact with the bipyridine. The volume of THF was reduced to 40 mL under dynamic vacuum and the solution was cooled to −20 °C, which resulted in the isolation of a small amount of green solid. The mother liquor was decanted into a Schlenk flask, the volume was reduced again and deep green crystals, which exhibit a very low solubility in toluene, pentane and diethyl ether, formed within 2 days at −20 °C. Yield: 2.38 g, 77%. Mp 218–220 °C. Anal. Calcd for $C_{20}H_{18}N_2$Yb: C, 52.3; H, 3.92; N, 6.10. Found: C, 52.3; H, 3,54; N, 6.08%. ^{1}H-NMR (C_6D_6, 23 °C): δ 53.1 (2H, $\nu_{\frac{1}{2}}$ = 50 Hz, bipy), 18.7 (2H, $\nu_{\frac{1}{2}}$ = 30 Hz, bipy), 10.8 (2H, $\nu_{\frac{1}{2}}$ = 30 Hz, bipy), 0.60 (2H, $\nu_{\frac{1}{2}}$ = 25 Hz, bipy), −1.69 (10H, $\nu_{\frac{1}{2}}$ = 9 Hz, C_5H_5). IR (Nujol mull; KBr windows; cm^{-1}): 1587 (m), 1566 (w), 1463 (s), 1431 (s), 1378 (m), 1271 (s), 1152 (m), 1055 (w), 1007 (s), 897 (w), 867 (w), 750 (vs), 729 (vs), 637 (w).

[1,2,4-$(Me_3Si)_3C_5H_2]_2$Yb. To a mixture of sodium tris(trimethylsilyl)cyclopentadienide[21] (2.33 g, 7.66 mmol) and YbI_2 (1.64 g, 3.83 mmol), tetrahydrofuran (150 mL) was added. The solution turned orange-red and was stirred at room temperature overnight. The solvent was removed under dynamic vacuum leaving a dark oily residue. This residue was exposed to dynamic vacuum for 5 hours at 40 °C, during which time the residue solidified and turned dark blue-green. The residue was extracted into pentane (100 mL), filtered and the solvent was removed under dynamic vacuum. The compound was purified by sublimation in diffusion pump vacuum at 80–90 °C and was then crystallised from pentane at −80 °C. Yield: 1.3 g (1.8 mmol, 46%). Mp 228–230 °C (rev.). Anal. Calcd for $C_{28}H_{58}Si_6Yb$: C, 45.67; H, 7.94. Found: C, 45.59; H, 8.09%. ^{1}H NMR (C_6D_6, 23 °C): δ 6.93 (4H, s, ring-C*H*), 0.42 (18 H, s, $SiMe_3$), 0.37 (36 H, s, $SiMe_3$). ^{13}C{^{1}H} NMR (C_6D_6, 23 °C): δ 132.5 (ring-*C*H), 130.8 (ring-*C*($SiMe_3$)), 125.9 (ring-*C*($SiMe_3$)), 1.78 ($SiMe_3$), 1.17 ($SiMe_3$). The EI mass spectrum showed a molecular ion at m/z = 736 amu. The parent ion isotopic cluster was simulated: (calcd%, observed%): 732 (5, 5), 733 (30, 31), 734 (61, 60), 735 (67, 66), 736 (100, 100), 737 (56, 57), 738 (54, 54), 739 (25, 26), 740 (12, 13), 741 (4, 4). IR (Nujol mull; CsI windows; cm^{-1}): 3042 (w), 1638 (vw), 1342 (w), 1250 (vs), 1140 (m), 1192 (vs), 1106 (s), 942 (s), 838 (br vs), 752 (s), 689 (m), 638 (m), 630 (sh), 510 (m), 439 (m), 398 (w), 377 (w), 368 (w), 306 (m), 235 (w). This reaction does not work well in diethyl ether, as the product was obtained in poor yield ($<$15%). This is probably due to the formation of [Cp′YbI(Et_2O)$_x$] (orange-red residue) as an intermediate which is not very soluble in pentane or toluene.[22] This residue disproportionates slowly on stirring in toluene at room temperature supporting this hypothesis.

[1,2,4-(Me_3Si)$_3C_5H_2$]$_2$Yb(bipy). 2,2′-Bipyridine (0.172 g, 1.09 mmol) was added to the base-free [1,2,4-(Me_3Si)$_3$-C_5H_2]$_2$Yb (0.80 g, 1.09 mmol) and the mixture was suspended in pentane (30 mL). The mixture turned dark green and was stirred at room temperature until the 2,2′-bipyridine dissolved completely. The solution was filtered, the solvent volume reduced, the flask was cooled to −80 °C resulting in the formation of dark blue-black crystals in 70% yield (0.68 g, 0.76 mmol). Mp 233–238 °C (dec.). Anal. Calcd for $C_{38}H_{64}N_2Si_6Yb$: C, 51.25; H, 7.24; N, 3.15. Found: C, 51.26; H, 7.55; N, 2.96%. ^{1}H NMR (C_6D_6, 23 °C): δ 9.16 (2H, d, $^3J_{HH}$ = 4.8 Hz, bipy), 7.47 (2H, “t”, $^3J_{HH}$ = 7.8 Hz, bipy), 6.99 (2H, d, $^3J_{HH}$ = 7.8 Hz, bipy), 6.81 (2H, “t”, $^3J_{HH}$ = 6.3 Hz, bipy), 6.73 (4H, s, ring-C*H*), 0.62 (18H, s, $SiMe_3$), 0.08 (36H, s, $SiMe_3$). IR (Nujol mull; CsI windows; cm^{-1}): 1595 (m), 1347 (w), 1320 (vw), 1305 (sh vw), 1262 (sh), 1250 (sh), 1242 (s), 1160 (m), 1092 (s), 1020 (sh), 1010 (m), 942 (s), 835 (br vs), 805 (sh), 762 (sh m), 752 (s), 725 (sh w), 682 (m), 640 (m), 625 (m), 510 (m), 435 (m), 378 (m), 358 (m), 292 (m).

[1,2,4-(Me_3C)$_3C_5H_2$]$_2$Yb(bipy). 2,2′-Bipyridine (0.244 g, 1.56 mmol) was added to base-free [1,2,4-(Me_3C)$_3C_5H_2$]$_2$Yb[23] (1.0 g, 1.56 mmol) and the mixture was dissolved in toluene (30 mL). The green-brown mixture turned dark brown and was stirred at room temperature for 30 min. The solution was filtered, the solvent volume reduced to 10 mL and the flask was cooled to −25 °C, resulting in the formation of large, dark red blocks in 64% yield (0.79 g, 0.99 mmol). The compound is sparingly soluble in aliphatic solvents and moderately soluble in benzene and toluene. Mp 172–178 °C (dec.). Anal. Calcd for $C_{44}H_{64}N_2Yb$: C, 66.39, H, 8.10, N, 3.52. Found: C, 66.40; H, 8.10; N, 3.49%. ^{1}H NMR (C_6D_6, 23 °C): δ 8.64 (br s, 4 H, $\nu_{\frac{1}{2}}$ = 55 Hz, bipy), 7.41 (br s, 2H, $\nu_{\frac{1}{2}}$ = 22 Hz, bipy), 6.69 (2H, dd, $^3J_{HH}$ = 5.5 Hz, $^3J_{HH}$ = 6.5 Hz, bipy), 5.97 (4H, s, ring-C*H*), 1.51 (18H, s, Me_3C), 1.42 (36H, s, Me_3C). IR (Nujol mull; CsI windows; cm^{-1}): 3088 (w), 1598 (m), 1578 (w), 1438 (m), 1360 (m), 1318 (w), 1302 (w), 1278 (w), 1240 (s), 1200 (w), 1165 (sh m), 1158 (m), 1105 (w), 1065 (w), 1048 (vw), 1023 (w), 1008 (w), 962 (w), 820 (w), 792 (s), 758 (vs), 740 (w), 732 (vw), 675 (m), 540 (m), 470 (w), 440 (vw), 428 (w).

{*ansa*-[2,4-(Me_3C)$_2C_5H_2$]$_2$SiMe$_2$}Yb(bipy). 2,2′-Bipyridine (0.070 g, 0.45 mmol) was added to the etherate of {*ansa*-[2,4-(Me_3C)$_2C_5H_2$]$_2$SiMe$_2$}Yb(OEt$_2$)[10] (0.30 g, 0.46 mmol) and the mixture was dissolved in toluene (30 mL). The volume was reduced slightly and the flask was cooled to −80 °C, resulting in the formation of dark blue crystals in 70% yield (0.23 g, 0.31 mmol). Mp 337–338 °C. Anal. Calcd for $C_{38}H_{54}N_2SiYb$: C, 61.7; H, 7.36; N, 3.79. Found: C, 60.5; H, 6.91; N, 3.16%. ^{1}H NMR (C_6D_6, 20 °C): δ 28.9 (2H, $\nu_{\frac{1}{2}}$ = 16 Hz, bipy or C_5H_2), 14.4 (2H, br. t, $\nu_{\frac{1}{2}}$ = 20 Hz, bipy), 10.1 (2H, $\nu_{\frac{1}{2}}$ = 11 Hz, bipy or C_5H_2), 9.2 (2H, $\nu_{\frac{1}{2}}$ = 17 Hz, bipy or C_5H_2), 5.08 (18H, $\nu_{\frac{1}{2}}$ = 8 Hz, Me_3C), 3.72 (2H, d, $^3J_{HH}$ = 6.4 Hz, bipy), 0.69 (18H, $\nu_{\frac{1}{2}}$ = 7 Hz, Me_3C), −0.05 (6H, $\nu_{\frac{1}{2}}$ = 7 Hz, Me_2Si), −2.15 (2H, $\nu_{\frac{1}{2}}$ = 10 Hz, bipy or C_5H_2). IR (Nujol mull; KBr windows; cm^{-1}): 1594 (w), 1461 (s), 1377 (s), 1154 (w), 1095 (w), 803 (w), 765 (w), 670 (w).

Acknowledgements

This work was supported by the Director, Office of Energy Research, Office of Basic Energy Sciences, Chemical Sciences Division of the U. S. Department of Energy under Contract No. DE-AC02-05CH11231. We thank the German Academic Exchange Service (DAAD) for a fellowship (M. D. W.) and W. W. Lukens and C. H. Booth for many hours of discussion.

References

1 M. Schultz, J. M. Boncella, D. J. Berg, T. D. Tilley and R. A. Andersen, *Organometallics*, 2002, **21**, 460–472.
2 D. J. Berg, J. M. Boncella and R. A. Andersen, *Organometallics*, 2002, **21**, 4622–4631.
3 C. H. Booth, M. D. Walter, M. Daniel, W. W. Lukens and R. A. Andersen, *Phys. Rev. Lett.*, 2005, **95**, 267202.
4 F. Weber, H. Sitzmann, M. Schultz, C. D. Sofield and R. A. Andersen, *Organometallics*, 2002, **21**, 3139–3146.
5 M. Schultz, C. J. Burns, D. J. Schwartz and R. A. Andersen, *Organometallics*, 2001, **20**, 5690–5699.
6 C. E. Zachmanoglou, A. Docrat, B. M. Bridgewater, G. Parkin, C. G. Brandow, J. E. Bercaw, C. N. Jardine, M. Lyall, J. C. Green and J. B. Keister, *J. Am. Chem. Soc.*, 2002, **124**, 9525–9546.
7 M. Kira, M. Watanabe and H. Sakurai, *J. Am. Chem. Soc.*, 1980, **102**, 5202–5207.
8 P. J. Barker, A. G. Davies and M.-W. Tse, *J. Chem. Soc., Perkin Trans. 2*, 1980, 941–948.
9 P. J. Barker, A. G. Davies, R. Henriquez and J.-Y. Nedelec, *J. Chem. Soc., Perkin Trans. 2*, 1982, 745–750.
10 M. Schultz, C. D. Sofield, M. D. Walter and R. A. Andersen, *New J. Chem.*, 2005, **29**, 919–927.
11 Y. Saito, J. Takemoto, B. Hutchinson and K. Nakamoto, *Inorg. Chem.*, 1972, **11**, 2003–2011.
12 C. J. O'Connor, in *Progress in Inorganic Chemistry*, ed. S. J. Lippard, J. Wiley & Sons, New York, 1982, vol. 29, pp. 203–285.
13 μ_{eff} values expressed in Bohr magnetons (μ_B) are related to those values expressed as χT by the expression $\chi T = (\mu_{eff}/2.828)^2$ in units of K cm^3 mol^{-1}.
14 E. König and S. Kremer, *Chem. Phys. Lett.*, 1970, **5**, 87–90.
15 R. E. Da Re, C. J. Kuehl, M. G. Brown, R. C. Rocha, E. D. Bauer, K. D. John, D. E. Morris, A. P. Shreve and J. L. Sarrao, *Inorg. Chem.*, 2003, **42**, 5551–5559.
16 R. D. Fischer, in *Organometallics of the f-elements: proceedings of the NATO Advanced Study Institute held at Sogesta, Urbino, Italy,*

September 11–22, 1978, ed. T. J. Marks and R. D. Fischer, D. Riedel Publishing Co., Dordrecht, 1979, p. 337.

17 R. D. Fischer, in *Fundamental and Technological Aspects of Organo-f-Element Chemistry*, ed. T. J. Marks and I. L. Fragala, D. Riedel Publishing Co., Dordrecht, 1985, p. 229.

18 G. Zi, L. Jia, E. L. Werkema, M. D. Walter, J. Gottfriedsen and R. A. Andersen, *Organometallics*, 2005, **24**, 4251–4264.

19 L. Maron, E. L. Werkema, L. Perrin, O. Eisenstein and R. A. Andersen, *J. Am. Chem. Soc.*, 2005, **127**, 279–292.

20 $(C5H5)_2Yb(bipy)$ also appears to exchange fast although the mechanism is probably different; the compound is not sufficiently soluble for more quantitative measurements.

21 M. A. Edelman, P. B. Hitchcock, J. Hu and M. F. Lappert, *New J. Chem.*, 1995, **19**, 481–489.

22 M. Schultz, PhD Thesis, University of California, Berkeley, 2000.

23 H. Sitzmann, T. Dezember, O. Schmitt, F. Weber, G. Wolmershäuser and M. Ruck, *Z. Anorg. Allg. Chem.*, 2000, **626**, 2241–2244.